Unfolding Pathway of the Dimeric and Tetrameric Forms of Phosphofructokinase-2 from *Escherichia coli*†

Mauricio Baez,‡ Ricardo Cabrera, Victoria Guixé, and Jorge Babul*

Departamento de Biología, Facultad de Ciencias Universidad de Chile, Casilla 653, Santiago, Chile

Received February 2, 2007; Revised Manuscript Received March 13, 2007

ABSTRACT: *Escherichia coli* phosphofructokinase-2 (Pfk-2) is an oligomeric enzyme characterized by two kinds of interfaces: a monomer−monomer interface, critical for enzymatic activity, and a dimer−dimer interface formed upon tetramerization due to allosteric binding of MgATP. In this work, Pfk-2 was denatured by guanidine hydrochloride (GdnHCl) and the impact of ligand binding on the unfolding pathway of the dimeric and the tertrameric forms of the enzyme was examined. The unligated dimeric form unfolds and dissociates from 0.15 to 0.8 M GdnHCl without the accumulation of native monomers, as indicated by circular dichroism and size exclusion chromatography measurements. However, a monomeric intermediate with an expanded volume and residual secondary structure accumulates above 0.8 M GdnHCl. The dimeric fructose-6-P−enzyme complex shows a shift in the simultaneous dissociation and unfolding process to elevated GdnHCl concentrations (from 0.8 to 1.4 M) together with the expulsion of the ligand detected by intrinsic fluorescence measurements. The unfolding pathway of the tetrameric MgATP−enzyme complex shows the accumulation of a tetrameric intermediate with altered fluorescence properties at about 0.4 M GdnHCl. Above this concentration a sharp transition from tetramers to monomers, without the accumulation of either compact dimers or monomers, was detected by light scattering measurements. Indeed, the most populated species was a partially unfolded monomer about 0.7 M GdnHCl. On the basis of these results, we suggest that the subunit contacts are critical for the maintenance of the overall structure of Pfk-2 and for the binding of ligands, explaining the reported importance of the dimeric state for enzymatic activity.

Quaternary structure, the three-dimensional arrangement of subunits, plays a critical role in the regulation, stability, and catalytic activity of oligomeric enzymes. In some cases, the interfacial contacts between subunits are completely required for proper function and stability of the oligomer. Such kinds of complexes have been referred to as permanent (*1*−*3*) because the isolation of their subunits in a correctly folded conformation that retains biological activity is difficult to achieve experimentally (for examples see refs *4*, *5*). On the other hand, the aggregation state of oligomeric enzymes can be modulated by protein−ligand interactions favoring subunit arrangements with different catalytic properties. In such cases, interfacial contacts participate principally in the regulatory mechanism of the enzymatic activity (*6*, *7*).

Phosphofructokinase activity is a major point of regulation in the central metabolic pathways of all organisms. In *Escherichia coli*, this activity is carried out by two nonhomologous (*8*) (structurally unrelated) oligomeric enzymes that depend on their intersubunit contacts for activity and regulation, phosphofructokinase-1 (Pfk-1[1]) and phosphofructokinase-2 (Pfk-2). Pfk-1 is a homotetramer (*9*) that shows activation by the allosteric binding of different effectors (*10*−*12*) and substrate-induced communication between the active sites in the oligomer (*13*). In the native Pfk-1 tetramer, two different interfaces contribute to the establishment of the substrates and effector sites, and their importance for catalysis and regulation has been extensively studied (*14*−*18*). Pfk-2 is a homodimer (*19*) of 66 kDa, which displays hyperbolic saturation kinetics for both substrates, fructose-6-P and MgATP (*20*). Hence, in opposition to Pfk-1, the active site in each monomer seems to work independently, i.e., without cooperative interactions, suggesting that monomer−monomer contacts in this enzyme should have evolved without the restrictions imposed by allosteric communication. Protein dilution and unfolding experiments show that dimer dissociation provokes the loss of the enzymatic activity (*21*), indicating a critical role of the intersubunit contacts for proper active site configuration. In this regard, Pfk-2 seems to work as a permanent complex, although it is unknown if enzyme inactivation occurs by subtle or profound structural changes in the monomer structure due to disruption of intersubunit contacts. Thus, knowledge of the physical properties of the dissociated monomer and its capacity to bind either fructose-6-P or MgATP should contribute to understanding of the role played by the monomer−monomer interface in the function of Pfk-2.

† Supported by a grant from the Comisión Nacional de Investigación Científica y Tecnológica, FONDECYT 1050818, Chile. M.B. is supported by Facultad de Ciencias, Universidad de Chile and FONDECYT.

* Corresponding author. Tel: (56 2) 978 7450. Fax: 56 2 272 6006. E-mail: jbabul@uchile.cl.

‡ Graduate student from the Facultad de Ciencias Químicas y Farmacéuticas, Universidad de Chile.

[1] Abbreviations: ANS, 8-anilino-1-naphthalene sulfonic acid; DTT, dithiotreitol; DLS, dynamic light scattering; GdnHCl, guanidine hydrochloride; Pfk-1, phosphofructokinase 1; Pfk-2, phosphofructokinase 2; R_h, hydrodynamic radius.

10.1021/bi7002247 CCC: $37.00
Published on Web 05/01/2007

On the other hand, in the presence of MgATP Pfk-2 dimers self-associate to produce homotetramers (*19*, *22*). This change has been associated with the inhibition of the enzymatic activity occurring at high concentrations of MgATP (*23*). In order to account for the observed effects, the binding of MgATP to an allosteric site has been proposed from enzyme kinetics and fluorescence experiments (*20*, *24*). Besides the constitution of a new interface, structural changes characterized by domain motions in the subunits are observed in the tetrameric MgATP-bound form of Pfk-2 (*22*). Also, overall compactation of the structure in the tetramer has been suggested from limited proteolysis experiments in the presence of MgATP (*25*). Although Caniuguir et al. (*21*) link the apparent stability of the tetramer to the inhibition mechanism, relevant intermediates resulting from GdnHCl denaturation in the presence of MgATP have not been characterized.

Because of the behavior described above, we consider Pfk-2 as a good model to evaluate the contribution of permanent (dimer) and ligand-modulated (tetramer) intersubunit interactions to the stability and function of oligomeric enzymes. The regulation of enzymatic activity by MgATP-induced inhibition in Pfk-2 has been demonstrated to be important for the growth of *E. coli* on gluconeogenic sources (*26*).

In this work, the unfolding pathways of the dimeric (free or fructose-6-P-bound) and tetrameric (MgATP-bound) forms of Pfk-2 were characterized through changes in enzymatic activity and structural properties by intrinsic fluorescence, circular dichroism, ANS binding, size exclusion chromatography, and dynamic light scattering measurements.

EXPERIMENTAL PROCEDURES

Pfk-2 Purification and Storage. E. coli Pfk-2 was purified and stored as described by Cabrera et al. (*25*). Previous to the unfolding or refolding experiments, the storage buffer was changed to the standard buffer (50 mM Tris pH 8.0, 5 mM $MgCl_2$, and 10 mM DTT) using a HiTrap desalting column (Amersham Biosciences, Uppsala, Sweden), following a 3 h dialysis in the same buffer. The enzyme was concentrated by using a Centricon-60 concentrator (Amicon, Beverly, MA). Protein concentration was determined by the Bradford assay (*27*).

Pfk-2 Unfolding. The unfolding studies were performed by diluting native Pfk-2 to several GdnHCl concentrations (Pierce, molecular biology grade) (*28*). Protein concentration ranged from 2 to 3 μM monomer unless otherwise indicated. The protein was incubated at several GdnHCl concentrations for 20 h at 20 °C. Under such conditions, control experiments revealed that nearly 90% of the original enzymatic activity was retained at 0 M GdnHCl, as well as the capacity to recover the original enzymatic activity when GdnHCl was diluted out from each starting concentration (data not shown).

Enzymatic Activity. Phosphofructokinase activity was measured spectrophotometrically by a coupled assay as described by Guixé et al. (*29*). The activity assay was started by dilution of a 1 μL aliquot containing the enzyme in GdnHCl into 700 μL of the assay mixture. Since this procedure implies the dilution of GdnHCl, renaturation should be expected to occur during the assay; however, control experiments show that reactivation was only 3% of the activity expected for the fully refolded protein during the time of measurement.

Intrinsic and ANS Fluorescence. Measurements were done in a Perkin-Elmer LS 50 spectrofluorimeter. Protein samples at several GdnHCl concentrations were excited at 295 nm to limit the fluorescence to the single tryptophan per monomer of Pfk-2 (Trp-88). Emission spectra were recorded from 300 to 480 nm using emission and excitation slits of 5 nm. The concentration of the stock solution of ANS (Molecular Probes, Eugene, OR) was determined using $\epsilon = 7800\ M^{-1}\ cm^{-1}$ at 372 nm in methanol. The Pfk-2 samples unfolded at different GdnHCl concentrations were incubated in 100 μM ANS for 3 h in the dark at 20 °C. The mixture was excited at 380 nm and the emission recorded from 400 to 580 nm.

Circular Dichroism Spectroscopy. Far UV CD spectra were acquired in a Jasco J600 dichrograph, employing a 1 mm cell. Each spectrum resulted from the accumulation of three scans (bandwidth 1 mm, scan rate 50 nm min^{-1}) between 210 and 260 nm (the high absorbance of 5−10 mM DTT did not allow the recording of spectra below 210 nm).

Size Exclusion Chromatography. Size exclusion chromatography equilibrium experiments were performed using a Water Breeze HPLC system equipped with a Supelco exclusion column (TSKgel G2000 SWXL 300 × 7.8 mm). The column was equilibrated with 60 mL of mobile phase containing 0.2 M KCl in standard buffer with the same GdnHCl concentration as that of the sample to be injected. The values of the column void volume (V_o) and total solvent-accessible column volume (V_t) were determined using the elution volumes (mL) of Blue dextran and DTT, respectively; the variation of V_o and V_t with the GdnHCl concentration was fitted to a linear equation: $V_o = 5.23 - 0.021 \times [GdnHCl]$ and $V_t = 12.21 - 0.176 \times [GdnHCl]$, respectively.

Dynamic Light Scattering Experiments (DLS). The hydrodynamic radius (R_h) of Pfk-2 in 50 mM Tris buffer pH 8, 5 mM $MgCl_2$, 10 mM DTT, incubated at different concentrations of GdnHCl for 20 h at 20 °C, was determined by DLS using a DynaPro MSTC014 (Protein Solutions, High Wycombe, Bucks, U.K.) at a protein concentration of 14 μM. All solutions were centrifuged at 13600*g* for 30 min prior to data collection. The protein concentration of the samples was measured before and after these treatments, and no significant loss of protein was observed. Data were acquired by accumulation of 18 readings of 5 s with detector sensitivity set to 80%. The particle size distribution was calculated by using the "regularization" method provided with the software DYNAMICS, supplied with the instrument. The residual scattering intensity (intensity scattered by the protein without solvent contribution) was also determined.

RESULTS

Enzymatic Activity, Intrinsic Fluorescence, and Circular Dichroism Measurements. The unfolding of Pfk-2 was induced by GdnHCl under three conditions, namely, 1 mM fructose-6-P, 1 mM MgATP, and without ligands, and the process was followed by enzymatic activity, intrinsic fluorescence, and circular dichroism measurements. Dissociation of dimeric Pfk-2 by GdnHCl has been previously correlated to the loss in enzymatic activity (*21*). Thus, we used enzymatic activity to follow the dimeric Pfk-2 that remains

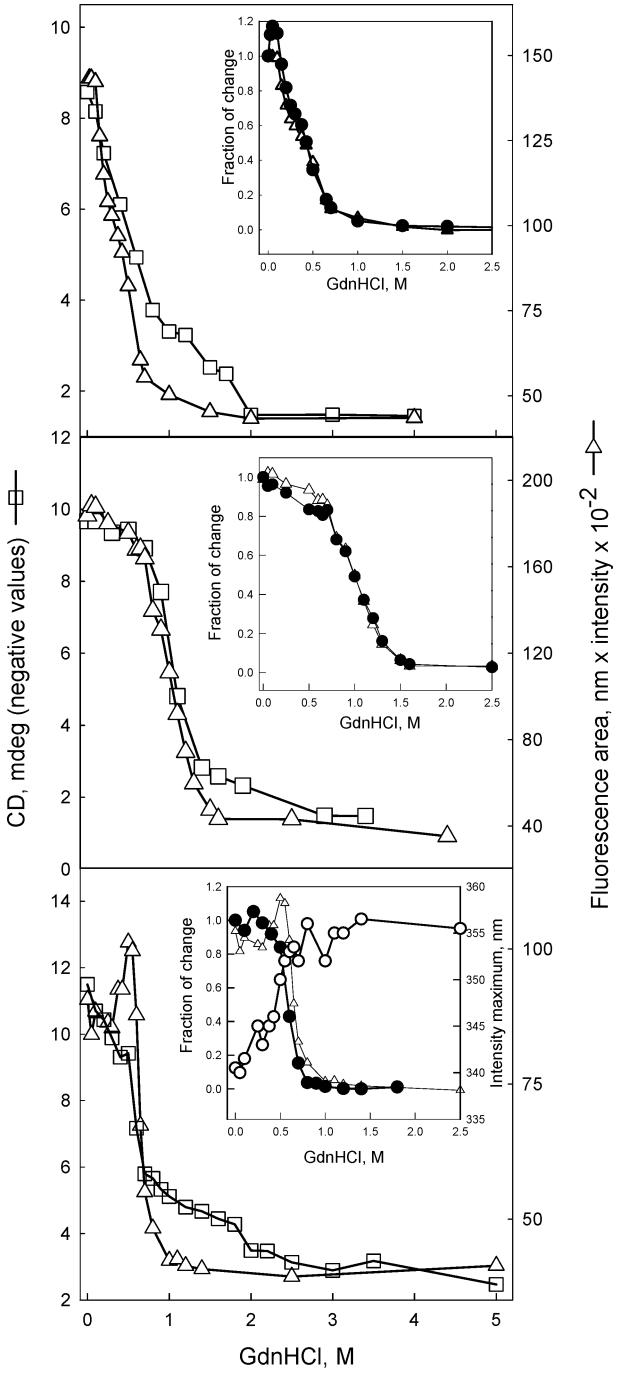

FIGURE 1: Effect of ligands in unfolding of Pfk-2 induced by GdnHCl. Pfk-2 unfolding was followed by measurements of enzymatic activity (●), area of the intrinsic fluorescence (△) and circular dichroism at 222 nm (□). Measurements for the free enzyme (panel A), with fructose-6-P 1 mM (panel B) or with MgATP 1 mM (panel C) are shown. For clarity the enzymatic activity was compared with the fluorescence area in each inset and expressed as fraction of change. Additionally, changes of the maximum emission of the intrinsic fluorescence signal (○) are compared in the inset of panel C.

during unfolding. In the same way, we used intrinsic fluorescence to monitor the changes in the structural environment of the single tryptophan per subunit (Trp-88). In the native state Trp-88 should be buried in a polar ambience, judging from the wavelength of maximum emission (λ_{max} = 350 nm; *24*).

In the absence of ligands (Figure 1A) the fluorescence area and enzymatic activity decrease together as a function of GdnHCl concentration up to about 0.8 M (Figure 1A, inset). Under the same conditions, the loss in the CD signal of the protein is not complete and an additional decrement is observed between 0.8 and 2 M GdnHCl (Figure 1A). Therefore, two transitions are involved in the unfolding of Pfk-2. The first one, between 0.15 and 0.8 M GdnHCl, accounts for the main change in secondary structure and the complete loss of native properties measured by enzymatic activity and intrinsic fluorescence. The second transition occurs between 0.8 and 2 M GdnHCl and accounts for the loss of the remaining amplitude of the CD signal measured at 222 nm.

Enzymatic activity is sensitive to Pfk-2 dissociation, whereas fluorescence is sensitive to fructose-6-P binding, increasing the intrinsic fluorescence of the free enzyme by about 30% (*24*). In the presence of fructose-6-P, the unfolding curves obtained by enzymatic activity and intrinsic fluorescence measurements superimpose into a single transition (Figure 1B, inset), coincident with the first step in the dichroic signal measured at 222 nm between 0.7 and 1.4 M GdnHCl. Above 1.4 M GdnHCl the CD signal decreases without changes in the intrinsic fluorescence and enzymatic activity, showing a not well-defined second transition with lower amplitude than the second transition observed for the free enzyme (compare Figures 1A and 1B).

Since only one transition is observed for the entire change in intrinsic fluorescence, the expulsion of fructose-6-P from the active site must be concomitant with the unfolding−dissociation step leading to the monomeric intermediate (compare the amplitudes of the fluorescence curves in Figure 1A and Figure 1B). Thus, the presence of 1 mM fructose-6-P shifts the first CD transition to higher GdnHCl concentrations, compared to the enzyme in the absence of the substrate, indicating the stabilization of the native dimeric enzyme by ligand binding to the active site (Figure 1B).

In the presence of MgATP the unfolding pathway starts from the homotetrameric form of Pfk-2. The tetramer−MgATP complex shows a 30% decrease in the fluorescence emission area and a shift of the emission maximum from 350 to 340 nm, relative to the free enzyme (*24*). The fluorescence-unfolding curve was complex showing at least three phases (Figure 1C). In the first phase, from 0 to 0.4 M GdnHCl, a red shift of the emission maximum occurs from 340 to about 350 nm without significant changes of the fluorescence area. Although this complexity was not evident through enzymatic activity measurements (inset, Figure 1C, black symbols), a rapid reconfiguration of the active site induced by the catalytic mixture cannot be ruled out under the enzymatic assay conditions. An increment of the fluorescence area was observed from 0.4 to about 0.5 M GdnHCl, followed by a sharp decrease ending at about 0.8 M GdnHCl (Figure 1C, open triangles). This sharp transition is also observed through enzymatic activity measurements and correlates well with an important loss of secondary structure (Figure 1C, open squares). The CD signal shows an additional transition above 0.7 M GdnHCl, indicating the presence of an intermediate with low content of secondary structure, as observed in the case of the free enzyme and in the presence of fructose-6-P.

As will be seen below, the first phase detected by the red shift of the emission maximum was not accompanied by the dissociation of the tetrameric MgATP complex, indicating

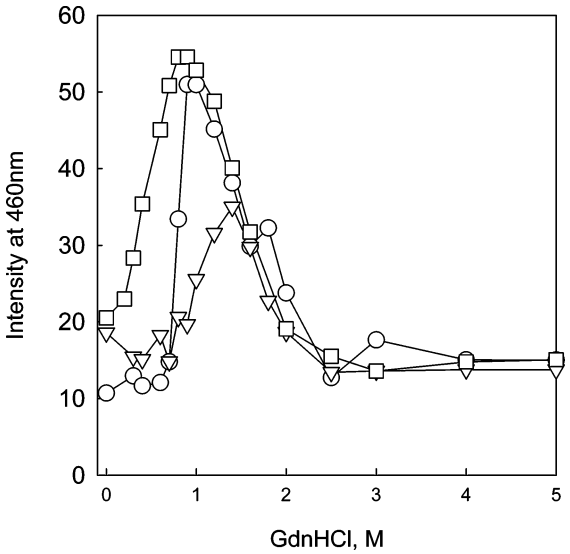

FIGURE 2: Changes in the ANS fluorescence during the unfolding of Pfk-2. ANS fluorescence was recorded at 460 nm for unfolding curves obtained without ligands (□), with 1 mM fructose-6-P (▽), or in the presence of 1 mM MgATP (○). The protein and the ANS concentrations were 2 μM and 100 μM, respectively.

the formation of a tetrameric additional intermediate around 0.4 M GdnHCl.

ANS Fluorescence Measurements. To further characterize the properties of the monomeric intermediate detected by circular dichroism, ANS was used in the unfolding solution as a sensitive probe for hydrophobic cavities in the protein (for example see ref *30*). Figure 2 shows the extrinsic fluorescence of the ANS measured at 460 nm at several GdnHCl concentrations. Without ligands, the ANS fluorescence increases, reaching a maximum value at approximately 0.8 M GdnHCl, and decreases at higher GdnHCl concentrations, reaching a minimal value at about 2 M. In the presence of MgATP, the ANS fluorescence intensity remains low and sharply increases above 0.6 M GdnHCl, reaching a maximum value at 0.9 M. This transition, although slightly shifted to higher denaturant concentrations, resembles the sharp transition that accounts for the major loss of the properties of the protein detected in the presence of MgATP. In the case of fructose-6-P, the increment of the ANS intensity occurs from 0.7 M to approximately 1.4 M GdnHCl, with a maximum value at half of the intensity observed for the free enzyme or the enzyme in the presence of MgATP. This result suggests that a minor population of intermediate coexists with the native dimer along the first transition detected by CD. Accordingly, stabilization by fructose-6-P shifts the intermediate formation toward higher GdnHCl concentration, where the unfolded state is favored, as indicated by the less apparent biphasic transition detected by CD. The results obtained with the ANS probe indicate that hydrophobic cavities in the intermediate(s) become more exposed to the solvent along the first transition detected by CD and unfold along the second transition.

Gel Filtration Chromatography Measurements. Size exclusion chromatography was used to determine changes in the hydrodynamic radius of the different species present in the unfolding pathway of Pfk-2. Figure 3 shows representative elution profiles of Pfk-2 obtained at several concentrations of the chaotrophic agent in the presence of 1 mM MgATP or 1 mM fructose-6-P or without ligands. Figure 4

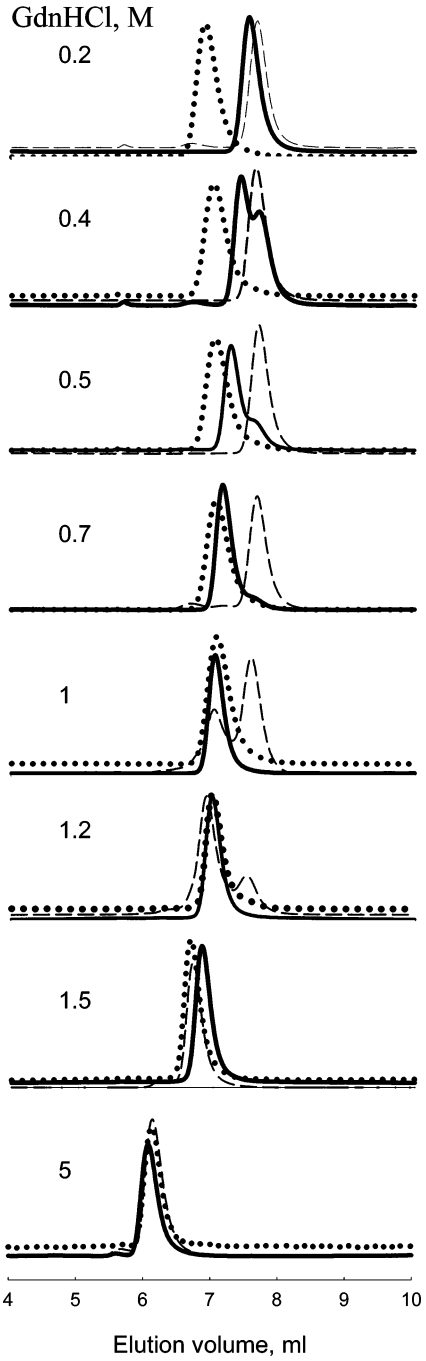

FIGURE 3: Elution profiles of Pfk-2 at different GdnHCl concentrations obtained by size-exclusion chromatography. Samples were injected into the column equilibrated with standard buffer containing 0.2 M KCl at the indicated GdnHCl concentrations plus 1 mM MgATP (dotted line) or 1 mM fructose-6-P (dashed line) or without ligands (solid line). Without ligands or with fructose-6-P the elution profiles were recorded at 280 nm, and with MgATP the elution profile was recorded at 295 nm. Molar concentrations of GdnHCl used to equilibrate the column are indicated for each chromatogram.

shows the observed elution volumes for the species detected in the chromatograms, plotted against the GdnHCl concentration.

In the absence of ligands, the elution volume of the protein increases with the GdnHCl concentration to a maximum value at 0.15 M (Figure 4A). This apparent diminution in the hydrodynamic radius was also observed in the presence of ligands, from 0 up to 0.7 M GdnHCl in the presence of fructose-6-P and from 0 to 0.4 M GdnHCl in the presence

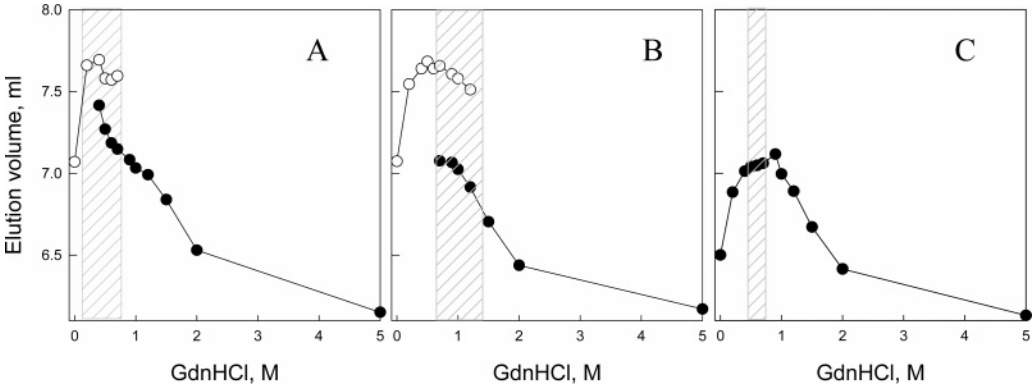

FIGURE 4: Effect of GdnHCl on the hydrodynamic properties of Pfk-2 in the presence and in the absence of ligands. Size-exclusion chromatography. Pfk-2 elution volume as a function of the GdnHCl concentration obtained without ligands (panel A), in the presence of 1 mM fructose-6-P (panel B), or with 1 mM MgATP (panel C). In A and B, the empty symbols represent the elution volume of the native-dimer species and the black symbols represent the elution volume for the "low elution volume species". In the presence of MgATP a single peak was observed during Pfk-2 unfolding (black symbols). The shaded zone represents the first transition region detected by spectroscopic techniques for each condition.

of MgATP (Figures 4B and 4C). However, control experiments performed at several salt concentrations indicate that this is an unspecific ionic-strength-induced effect and does not reflect changes in the aggregation state of the protein.

As shown in Figure 3, in the absence of ligands an additional peak coexists with the native dimer peak from 0.2 to 0.8 M GdnHCl but with a lower elution volume (Figure 3, continuous line). In the presence of fructose-6-P, the additional peak appears beyond 0.7 M GdnHCl and coexists with the native peak up to 1.3 M (Figure 3, dashed line) while in the presence of MgATP no additional peaks are apparent from the elution profiles (Figure 3, dotted line).

The plot of the elution volume of the species separated by the column in the absence of ligands (Figure 4A) and in the presence of fructose-6-P (Figure 4B) was compared with the GdnHCl concentrations intervals (see the shaded zone in Figure 4, panels A and B) where the first transition associated with the formation of the monomeric intermediate occurs under both conditions (Figures 1A and 1B). The native-dimer peak (open symbols) and the low elution volume additional peak (closed symbols) can only be detected in these GdnHCl concentration intervals, suggesting that the additional peak represents the monomeric intermediate. Indeed, the injection of samples with increasing protein concentrations from 1 to 18 μM into the column equilibrated with 0.3 M GdnHCl shows an increment in the population of the native peak relative to the additional peak, as expected from the mass action principle (data not shown). Therefore, the additional peak represents a monomer with an expanded volume larger than the native dimer since it has an elution volume lower than the native peak. The observation of distinct peaks for the dimer and expanded monomer suggests that both species interconvert slowly on the time scale of the chromatographic separation.

On the other hand, in the absence of GdnHCl a diminution in the elution volume is observed as a consequence of the MgATP-induced tetramerization (Figure 3 and Figure 4C). Between 0 and 0.4 M GdnHCl, the elution volume of the protein increases (Figure 4C), but tetramer dissociation is unlikely to occur since the elution volume is lower than the one corresponding to a compact dimer under the same conditions (see Figure 3 at 0.4 M GdnHCl). The dashed zone in Figure 4C represents the interval of GdnHCl concentrations where the major changes in the structural properties of Pfk-2 are expected in the presence of MgATP. However the elution volume observed in this interval remains almost unchanged, and no other species were apparent from the chromatograms. Thus, correlations of elution volumes with tetramer dissociation or unfolding are difficult to establish. Beyond the transition zone shown in each condition, in the absence of ligands, in the presence of fructose-6-P, and in the presence of MgATP, Pfk-2 experiences a diminution of the elution volume and an increment of its R_h upon further increasing the GdnHCl concentration. This behavior was similar for the three conditions studied, indicating that the intermediate species further unfolds irrespective of the presence of ligands. This process can also be observed as a diminution of the ANS intensity after reaching its maximum (Figure 2) or as the second transition detected by CD for each experimental condition (Figure 1).

Dynamic Light Scattering Measurements. Dynamic light scattering measurements were used as a complementary methodology to determine the hydrodynamic changes along tetramer unfolding given the difficulty in interpreting the elution profile obtained by size exclusion chromatography as a function of the GdnHCl concentration in the presence of MgATP (see above). This methodology allows the simultaneous measure of the molecular weight of the particle and the hydrodynamic radius (R_h) associated with the dissociation and unfolding processes (*30*, *31*).

At 0 M GdnHCl, the MgATP−Pfk-2 complex shows an R_h value of 4.31 ± 0.025 nm (about 8 nm higher than the native dimer). This value and the scattered intensity remain almost constant to about 0.4 M GdnHCl (Figure 5). These results indicate that the tetramer configuration remains intact under these conditions and that the elution volume increment observed by size exclusion chromatography is due to unspecific salt-induced interactions with the column.

Above 0.4 M GdnHCl the R_h decreases from 4.31 ± 0.025 (native tetramer) to a minimum value of 3.76 ± 0.07 measured at 0.7 M GdnHCl (Figure 5). Beyond 0.7 M GdnHCl the R_h value shows an increment reaching a value of 4.6 ± 0.19 nm at 3 M GdnHCl. The overall change in the scattered intensity was observed between 0.4 and 0.7 M GdnHCl, showing that tetramer dissociation to monomers was complete at about 0.7 M GdnHCl. Given that a 33 kDa

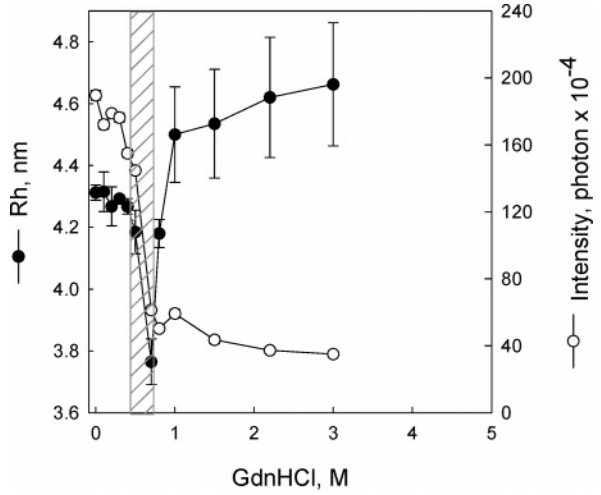

FIGURE 5: Hydrodynamic changes followed by dynamic light scattering. The enzyme was unfolded in the presence of 1 mM MgATP, and the intensity of the dispersed light was recorded (○). The hydrodynamic radius (●) for each sample was calculated from the autocorrelation function obtained from an autocorrelator of 248 channels. The error bars were calculated from 4 measurements. Samples were centrifuged at 13000*g* before the measurements. Protein concentration was 14 μM.

folded globular monomer should have an R_h of 2.5 nm (*32*, *33*) and that the minimal R_h value obtained at 0.7 M of GdnHCl was 3.76 nm, a compact monomer seems not highly populated throughout tetramer dissociation induced by GdnHCl. This assumption is also supported by the good correlation between tetramer dissociation and the CD changes observed in this interval of chaotrophic agent (Figure 5, shaded zone). The R_h increment observed above 0.7 M GdnHCl in the presence of MgATP suggests that the unfolding of the monomeric intermediate correlates well with the second CD transition detected beyond 0.7 M GdnHCl (Figure 1C).

DISCUSSION

The unfolding of the Pfk-2 initiated from its dimeric state (without ligands or in the presence of fructose-6-P) or from its tetrameric state (in the presence of MgATP) was characterized by several methodologies. The hallmark of populated intermediates present in the unfolding pathway of proteins is the lack of superposition between the unfolding curves detected by several methodologies and/or unfolding curves with more than one transition. In the case of Pfk-2 unfolding in the absence of ligands there is a lack of superposition between the unfolding curves obtained by CD and the unfolding curves obtained from intrinsic fluorescence and enzymatic activity measurements. These observations support the presence of at least one intermediate in the unfolding pathway of the protein. The structural properties of this intermediate can be inferred at 0.8 M of GdnHCl since CD measurements show residual secondary structure in spite of the complete loss of the enzymatic activity and intrinsic fluorescence, suggesting the presence of a somewhat unfolded species. Additional information was obtained from the ANS extrinsic fluorescence which was maximal at 0.8 M GdnHCl indicating the presence of hydrophobic cavities in the intermediate. This characteristic contrasts with the classical molten globule characterized by a large content of secondary structure (*34*), since the ANS maximum intensity was observed about 0.8 M GdnHCl where the CD unfolding curve shows a low content of secondary structure. The presence of the intermediate could also be detected by measuring the hydrodynamic changes of the protein by size exclusion chromatography. In the absence of ligands an additional peak with a hydrodynamic radius larger than the native dimer was observed. Since previous studies indicates that Pfk-2 dissociation can be correlated with the enzymatic activity (*21*), the low elution volume additional peak should be a monomer since this species was formed along the transition showing the loss of enzymatic activity. This assumption was confirmed by injecting samples of increasing protein concentrations to the column. The large R_h of the monomer can be explained by the polypeptide unfolding, as deduced from the major loss in secondary structure (about 70% of the native CD signal) observed along with the apparition of the low elution volume additional peak. The observation of two species in the chromatograms, the dimer and the monomeric intermediate, along with the considerable loss of secondary structure that occurs with the formation of the intermediate, suggests a strong coupling between interface interactions and subunit stability. Obligated or permanent complexes characterized by large interfaces dominated by hydrophobic contacts present high coupling between the dissociation and unfolding processes (*35*), which accounts for a large part of the whole stabilization energy of these proteins (*36*). In this kind of complex the interfacial interactions are characterized by physical and chemical properties that resemble those present in the hydrophobic core of the proteins, making the interface itself a compact structural domain in the protein (*2*, *3*). Recently, crystals were obtained from the tetrameric MgATP-bound form of Pfk-2 (*37*) and the solved structure (manuscript in preparation) indicates a strong resemblance with the edge-to-edge dimers of the ribokinase superfamily of sugar kinases to which Pfk-2 belongs (*38*). The interface in these dimers is characterized by the orthogonal packing of a four-stranded beta-sheet domain, characterized by a large and highly intertwined interface dominated by hydrophobic interactions (*38*, *39*).

The incorporation of fructose-6-P in the unfolding mixture displaces the dissociation−unfolding process to higher GdnHCl concentrations, suggesting the stabilization of a dimeric conformation by fructose-6-P binding (Figure 1B). In support of this observation, size-exclusion experiments in the presence of fructose-6-P show that the monomeric intermediate along the unfolding pathway of Pfk-2 is less populated than in the case of the free enzyme (see, for example, at 1 M GdnHCl, Figure 3). This is consistent with a lower ANS intensity (Figure 2) and a not well-defined second transition (Figure 1B) than in the absence of substrates. Therefore, the binding of fructose-6-P does not induce the accumulation of new intermediates, as it was observed with Pfk-1 (*17*). In that case, fructose-6-P cross-links the Pfk-1 tetramer allowing conformational changes into each subunit prior to dissociation.

In the presence of MgATP, the tretramer unfolding measured by dynamic light scattering shows that from 0 to 0.4 M GdnHCl the tetramer does not dissociate. However, a shift in the fluorescence maximum emission was detected in this interval of GdnHCl concentration suggesting the presence of a tetrameric intermediate. Tetramer dissociation to an expanded mononomeric intermediate occurs in a short

interval of GdnHCl concentrations, as shown by DLS measurements. At 0.7 M GdnHCl the R_h reaches a minimum value of 3.76 nm suggesting the absence of compact MgATP-bound monomers. The low content of secondary structure obtained at 0.7 M GdnHCl supports this suggestion. The sharp transition detected in the course of tetramer dissociation argues against the presence of another species like compact MgATP-bound dimer, indicating that tetramer dissociation occurs as an all-or-nothing process. In fact, other properties associated with the dissociation of the tetramer (intrinsic fluorescence, CD, and enzymatic activity) show very sharp transitions. This behavior can be explained by the increment of accessible surface area buried upon tetramer formation that predicts an increment of the sensitivity toward the chaotropic agent (*40*). The absence of compact dimers as unfolding intermediates suggests that the stabilization of the protein by nucleotide binding requires the establishment of the quaternary contacts present in the tetramer. Given its marginal stability, the eventual presence of these species should readily produce the expanded monomeric intermediate. In this regard, evidence for structural effects besides tetramer formation has been obtained from small-angle X-ray scattering (*22*) and limited proteolysis studies (*25*). These conformational changes were described as domain motions and global compaction of the subunit. Thus, we can conclude that the conformational changes triggered by MgATP must be strongly coupled with the formation of interfacial contacts between dimers. On the other hand, a survey performed with structures of transient oligomers (*41*) shows that the "strongest" interfaces belong to transient oligomers triggered by ligands, whose contact properties are closer to those of the obligated oligomers than the weak transient complexes driven by mass action. The tetramer conformation can be an extreme case of transient oligomers triggered by ligands since tetramer conformation cannot be reached by increments of the protein concentration even up to 30 mg/mL of Pfk-2 (unpublished observations). This result suggests that tetramer formation occurs by a sequential mechanism that involves the interaction of two dimer−MgATP complexes since association between free dimers has not been observed. The strong coupling between the conformational changes induced by MgATP binding and dimer−dimer interaction suggests that a dimer−MgATP complex is marginally populated. Therefore, and considering that the ATP concentration inside the bacterium is around 3 mM (*42*), far over the K_d calculated for the MgATP induced tetramerization, the tetramer could be the predominant form of Pfk-2 under physiological conditions. However, other factors, such as the fructose-6-P concentration under different metabolic conditions, play a role in tetramer formation (*23*, *26*). The expression in *E. coli* of a mutant Pfk-2 not inhibited by MgATP, which is unable to form tetramers, impairs the growth on gluconeogenic sources (*26*).

ACKNOWLEDGMENT

We thank Patricio H. Rodríguez for valuable help during the initial stages of this work and Octavio Monasterio for the use of the spectropolarimeter

REFERENCES

1. Jones, S., and Thornton, J. M. (1996) Principles of protein-protein interactions, *Proc. Natl. Acad. Sci. U.S.A. 93*, 13−20.
2. Jones, S., Marin, A., and Thornton, J. M. (2000) Protein domain interfaces: characterization and comparison with oligomeric protein interfaces, *Protein. Eng. 13*, 77−82.
3. Tsai, C. J., and Nussinov, R. (1997) Hydrophobic folding units at protein-protein interfaces: implications to protein folding and to protein-protein association, *Protein. Sci. 6*, 1426−1437.
4. Beernink, P. T., and Tolan, D. R. (1996) Disruption of the aldolase A tetramer into catalytically active monomers, *Proc. Natl. Acad. Sci U.S.A. 93*, 5374−5379.
5. Najera, H., Costas, M., and Fernandez-Velasco, D. A. (2003) Thermodynamic characterization of yeast triosephosphate isomerase refolding: insights into the interplay between function and stability as reasons for the oligomeric nature of the enzyme, *Biochem. J. 370*, 785−792.
6. Kim, J., and Raushel, F. M. (2001) Allosteric control of the oligomerization of carbamoyl phosphate synthetase from *Escherichia coli*, *Biochemistry 40*, 11030−11036.
7. Kashlan, O. B., Scott, C. P., Lear, J. D., and Cooperman, B. S. (2002) A comprehensive model for the allosteric regulation of mammalian ribonucleotide reductase. Functional consequences of ATP- and dATP-induced oligomerization of the large subunit, *Biochemistry 41*, 462−474.
8. Ronimus, R. S., and Morgan, H. W. (2001) The biochemical properties and phylogenies of phosphofructokinases from extremophiles, *Extremophiles 5*, 357−373.
9. Shirakihara, Y., and Evans, P. R. (1988) Crystal structure of the complex of phosphofructokinase from *Escherichia coli* with its reaction products, *J. Mol. Biol. 204*, 973−994.
10. Blangy, D., Buc, H., and Monod, J. (1968) Kinetics of the allosteric interactions of phosphofructokinase from *Escherichia coli*, *J. Mol. Biol. 31*, 13−35.
11. Rypniewski, W. R., and Evans, P. R. (1989) Crystal structure of unliganded phosphofructokinase from *Escherichia coli*, *J. Mol. Biol. 207*, 805−821.
12. Babul, J. (1978) Phosphofructokinases from *Escherichia coli*. Purification and characterization of the nonallosteric isozyme, *J. Biol. Chem. 253*, 4350−4355.
13. Fenton, A. W., and Reinhart, G. D. (2003) Mechanism of substrate inhibition in *Escherichia coli* phosphofructokinase, *Biochemistry 42*, 12676−12681.
14. Martel, A., and Garel, J. R. (1984) Renaturation of the allosteric phosphofructokinase from *Escherichia coli*, *J. Biol. Chem. 259*, 4917−4921.
15. Bras, G. L., Teschner, W., Deville-Bonne, D., and Garel, J. R. (1989) Urea-induced inactivation, dissociation, and unfolding of the allosteric phosphofructokinase from *Escherichia coli*, *Biochemistry 28*, 6836−6841.
16. Deville-Bonne, D., Le Bras, G., Teschner, W., and Garel, J. R. (1989) Ordered disruption of subunit interfaces during the stepwise reversible dissociation of *Escherichia coli* phosphofructokinase with KSCN, *Biochemistry 28*, 1917−1922.
17. Teschner, W., Deville-Bonne, D., and Garel, J. R. (1990) Fructose-6-phosphate modifies the pathway of the urea-induced dissociation of the allosteric phosphofructokinase from *Escherichia coli*, *FEBS. Lett. 267*, 96−98.
18. Quinlan, R. J., and Reinhart, G. D. (2006) Effects of protein-ligand associations on the subunit interactions of phosphofructokinase from *B. stearothermophilus*, *Biochemistry 45*, 11333−11341.
19. Kotlarz, D., and Buc, H. (1981) Regulatory properties of phosphofructokinase 2 from *Escherichia coli*, *Eur. J. Biochem. 117*, 569−574.
20. Campos, G., Guixé, V., and Babul, J. (1984) Kinetic mechanism of phosphofructokinase-2 from *Escherichia coli*. A mutant enzyme with a different mechanism, *J. Biol. Chem. 259*, 6147−6152.
21. Caniuguir, A., Cabrera, R., Baez, M., Vásquez, C. C., Babul, J., and Guixé, V. (2005) Role of Cys-295 on subunit interactions and allosteric regulation of phosphofructokinase-2 from *Escherichia coli*, *FEBS. Lett. 579*, 2313−2318.
22. Cabrera, R., Fischer, H., Trapani, S., Craievich, A. F., Garratt, R. C., Guixé, V., and Babul, J. (2003) Domain motions and quaternary packing of phosphofructokinase-2 from *Escherichia coli* studied by small angle x-ray scattering and homology modeling, *J. Biol. Chem. 278*, 12913−12919.
23. Guixé, V., and Babul, J. (1988) Influence of ligands on the aggregation of the normal and mutant forms of phosphofructokinase 2 of *Escherichia coli*, *Arch. Biochem. Biophys. 264*, 519−524.
24. Guixé, V., Rodríguez, P. H., and Babul, J. (1998) Ligand-induced conformational transitions in *Escherichia coli* phosphofructokinase

2: evidence for an allosteric site for MgATP2, *Biochemistry 37*, 13269−13275.
25. Cabrera, R., Guixé, V., Alfaro, J., Rodriguez, P. H., and Babul, J. (2002) Ligand-dependent structural changes and limited proteolysis of *Escherichia coli* phosphofructokinase-2, *Arch. Biochem. Biophys. 406*, 289−295.
26. Torres, J. C., Guixe, V., and Babul, J. (1997) A mutant phosphofructokinase produces a futile cycle during gluconeogenesis in *Escherichia coli*, *Biochem. J. 327*, 675−684.
27. Bradford, M. M. (1976) A rapid and sensitive method for the quantitation of microgram quantities of protein utilizing the principle of protein-dye binding, *Anal. Biochem. 72*, 248−254.
28. Pace, C. N. (1986) in *Enzyme Structure, Part L* (Hirs, C. H. W., and Timasheff, S. N., Eds.) pp 266−280, Academic Press, Inc., New York.
29. Guixé, V., and Babul, J. (1985) Effect of ATP on phosphofructokinase-2 from *Escherichia coli*. A mutant enzyme altered in the allosteric site for MgATP, *J. Biol. Chem. 260*, 11001−11005.
30. Sanyal, S. C., Bhattacharyya, D., and Das Gupta, C. (2002) The folding of dimeric cytoplasmic malate dehydrogenase. Equilibrium and kinetic studies, *Eur. J. Biochem. 269*, 3856−3866.
31. Asgeirsson, B., Hauksson, J. B., and Gunnarsson, G. H. (2000) Dissociation and unfolding of cold-active alkaline phosphatase from atlantic cod in the presence of guanidinium chloride, *Eur. J. Biochem. 267*, 6403−6412.
32. Uversky, V. N. (1993) Use of fast protein size-exclusion liquid chromatography to study the unfolding of proteins which denature through the molten globule, *Biochemistry 32*, 13288−13298.
33. Uversky, V. N. (2002a) What does it mean to be natively unfolded?, *Eur. J. Biochem. 269*, 2−12.
34. Uversky, V. N. (2002b) Natively unfolded proteins: a point where biology waits for physics, *Protein. Sci. 11*, 739−756.
35. Larsen, T. A., Olson, A. J., and Goodsell, D. S. (1998) Morphology of protein-protein interfaces, *Structure 6*, 421−427.
36. Neet, K. E., and Timm, D. E. (1994) Conformational stability of dimeric proteins: quantitative studies by equilibrium denaturation, *Protein. Sci. 3*, 2167−2174.
37. Cabrera, R., Caniuguir, A., Ambrosio, A. L., Guixé, V., Garratt, R. C., and Babul, J. (2006) Crystallization and preliminary crystallographic analysis of the tetrameric form of phosphofructokinase-2 from *Escherichia coli*, a member of the ribokinase family, *Acta Crystallogr., Sect. F: Struct. Biol. Cryst. Commun. 62*, 935−937.
38. Zhang, Y., Dougherty, M., Downs, D. M., and Ealick, S. E. (2004) Crystal structure of an aminoimidazole riboside kinase from *Salmonella enterica*: implications for the evolution of the ribokinase superfamily, *Structure 12*, 1809−1821.
39. Sigrell, J. A., Cameron, A. D., Jones, T. A., and Mowbray, S. L. (1998) Structure of *Escherichia coli* ribokinase in complex with ribose and dinucleotide determined to 1.8 A resolution: insights into a new family of kinase structures, *Structure 6*, 183−193.
40. Fersht, A. (1998) *Structure and Mechanism in Protein Science: A Guide to Enzyme Catalysis and Protein Folding*, 2nd ed., pp 508−540, W. H. Freeman, New York.
41. Nooren, I. M., and Thornton, J. M. (2003) Structural characterization and functional significance of transient protein-protein interactions, *J. Mol. Biol. 325*, 991−1018.
42. Schneider, D. A., and Gourse, R. L. (2004) Relationship between growth rate and ATP concentration in *Escherichia coli*, *J. Biol. Chem. 279*, 8262−8268.

BI7002247